All that glitters is not BOLD: inconsistencies in functional MRI

Ville Renvall, Cathy Nangini, Riitta Hari

Supplementary Information

Methods

Data analysis

Time course analysis (Figures 4 and S3)

The concatenated runs were corrected for motion and realigned to the first data point of the FA12/TE30-scan, (using spm8 software, http://www.fil.ion.ucl.ac.uk/spm/). Matlab (version 7.9.0.529, The MathWorks, Natick, MA, USA) scripts were used for the remainder of the analysis. While the spm default parameters were retained in the final analysis, for comparison, several different parameters were tried for motion correction, and the step was also repeated with AFNI: the resulting time series data were essentially the same in the within-brain voxels. First-order intensity trends were removed from each concatenated run by fitting a line to the 8-s control periods immediately preceding the stimulation. Percent signal changes (%Δ*S*) were obtained by subtracting the mean of the detrended 8-s control periods from the signal value and dividing by the same mean for each time point separately. %Δ*S* from the four trials were averaged. Interpolation to 10 sections of cubic splines was utilized to trade temporal resolution for noise reduction. Fitting the 10-section splines of equal duration to the data (now 56 s = 70 time points) kept the dynamics of the data without introducing new features or imposing any model, except the requirement that the spline sections be sufficient to capture the true waveform adequately.

The spline-interpolated time courses of the six *FA*/*TE* combinations were plotted for every brain voxel in an image plane (plane 11/14 in Fig. 4, chosen to be far from the edge of the image stack, *sinus rectus*, and ventricles to avoid artifacts), overlaid on the gray value of the FA12/TE30-scan for anatomical reference. To improve the visibility of the time course traces, the background image (in Fig. 1B) was "whitewashed" with a layer of white at 30 % opacity.

The individual time course plots were amplitude-scaled voxel-by-voxel so that the minimum dynamics of signal change was set to ±2 % (in which case the scale-indicating dark-gray bar extends from the top to the bottom of the plot), but if greater scale was required, the range was increased (indicated by a shorter bar). The width of the bar shows the duration of the checkerboard stimulation.

The reference images displayed are the mean across two time points preceding the first stimulation period at each *FA*.

Scatter plots (Figure S1 and Tables S1–S2)

Statistically significantly activated voxels ($p < 0.05$, FDR-corrected) in the task-related activation analysis were extracted from the left-hemisphere ROIs. Fig. 1 shows the scatter plots of data of two ROIs for all subjects for FA12 vs. FA90. Tables S1 and S2 contain the same data grouped into positive and negative activations.

tSNR analysis (Figure S2)

Temporal signal-to-noise ratio (tSNR) was calculated for the four concatenated runs produced for all *FA*s in the preprocessing pipeline before the intensity normalization step. Here, instead of intensity normalization, the concatenated runs were detrended for linear drift, transformed into Talairach space, then the time series data were extracted for each ROI. The tSNR, defined as S/σ, where S = mean voxel time course and σ = its standard deviation, was calculated voxel-wise by averaging data within the baseline windows only (14 s before the onset of each stimulus block). Points in the baseline window with excessive motion were excluded, as described in Methods. The mean tSNR across all voxels in each ROI for all *FA* conditions was then computed. The ROI means were then averaged across all 8 subjects. Fig. S2 shows the region-specific tSNR (± SEM) for FA12 and FA90.

Noise distributions (Figure S4)

As noise and physiological fluctuations in the brain are not necessarily uniformly distributed across voxels, stimulation time course, and *FA*, we inspected the statistically significantly responding voxels in several ROIs for differences of skewness in the noise distributions between the stimulation and control conditions at different *FA*s, because noise skew could introduce activation-like changes.

Pools of samples were extracted roughly from the plateau periods of the measured time series such that the last ~13 s and ~9 s of data were included in the control and stimulation pools from each trial, respectively, with the exact number of time points depending on the *TR*. From these pooled data points for the control and stimulation periods, a random sample of 1000 points was bootstrapped from each responding voxel and the skewness was calculated. Scatter plots of the median skewness of the control vs. stimulation periods were plotted for each voxel separately for each *FA* and visually inspected. Figure S4 shows these plots for a representative subject (S4) for (clockwise from upper left) V1, precuneus, cuneus and PCC.

Seed analysis (Table S3)

Individual subject activation maps for each *FA* condition were calculated using a reference waveform that consisted of the average time series (smoothed using a five-point moving average and detrended) obtained from all voxels in the left V1 ROI. Table S3 shows the total number (summed across all 8 subjects) of positive and negative significantly activated voxels in all left-hemisphere ROIs (excluding left primary visual cortex, the seed ROI).

Supplementary Information

Results

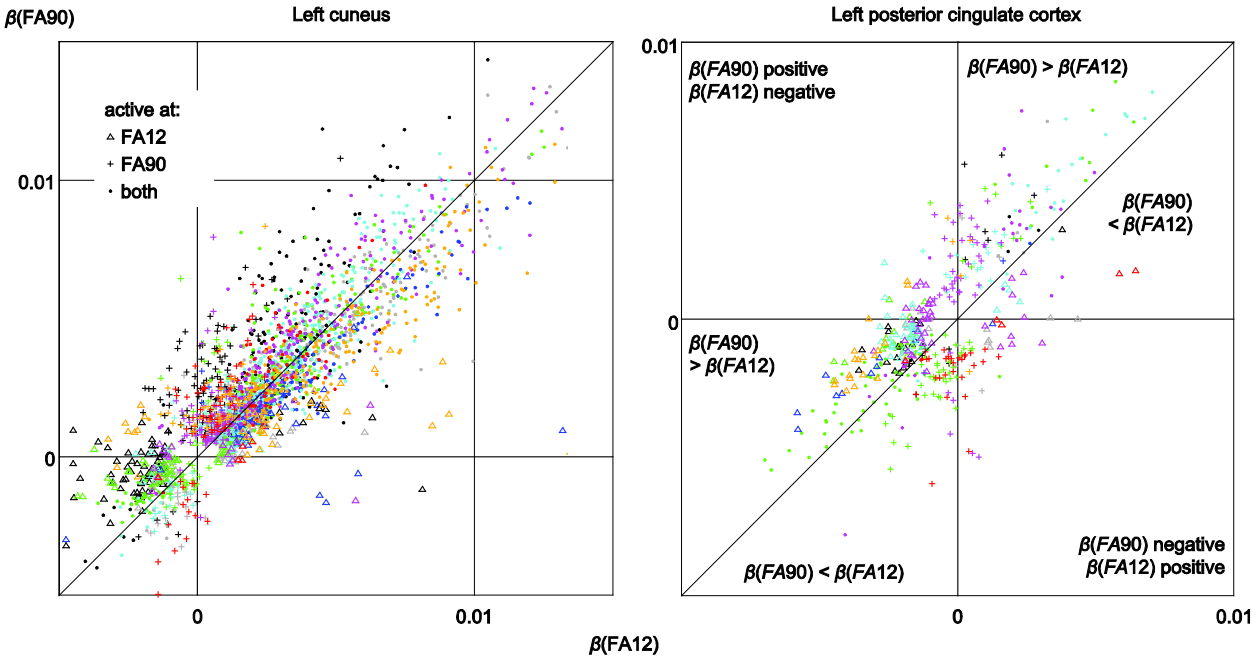

Fig. S1. *FA* effects on task-related activations. Scatter plots of beta coefficients of significantly activated voxels ($p < 0.05$, FDR-corrected) extracted from two left-hemisphere ROIs, pooled across all 8 subjects, for FA12 vs FA90. Triangles indicate voxels active only for FA12, pluses for FA90, and small dots represent voxels active for both *FA*s. The eight colors represent the data from the eight different subjects. The distribution of significantly activated voxels was quite similar for the two *FA*s in the *FA*-insensitive cuneus, but the distributions were dissimilar in *FA*-sensitive PCC: e.g. the number of negatively activated voxels at FA12 clearly outnumbers the positive ones, whereas at FA90, the proportions are more even. Cropping of the figures excluded 38 points of data from cuneus and 2 from PCC.

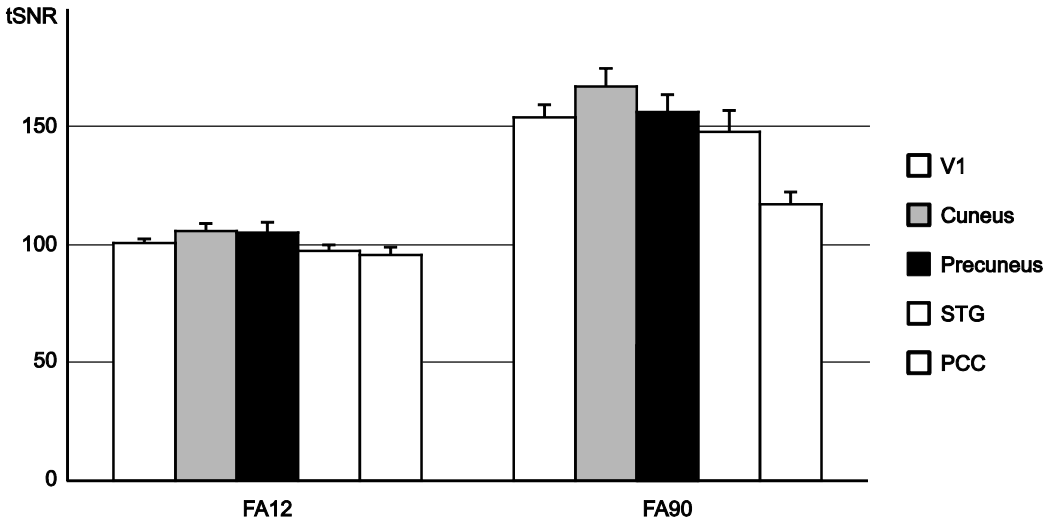

Fig. S2. Region-specific temporal signal-to-noise analysis. Mean tSNR obtained by dividing the fMRI time course means by the noise, voxel-wise, then averaging across subjects.

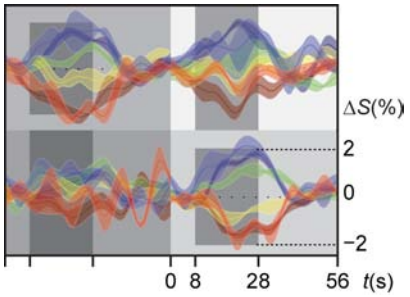

Fig. S3. CSF effect. Signal time courses of four neighboring voxels located partially within a ventricle (the bright upper-right voxel of the image is mostly within the ventricle) illustrate the sustained CSF effect during stimulation. Note that the blue and red data were acquired within a single run, green and yellow traces in another run, and violet and brown traces in yet another run; these pairs are thus the most comparable in terms of subject alertness and co-location. Bands: mean ± SEM.

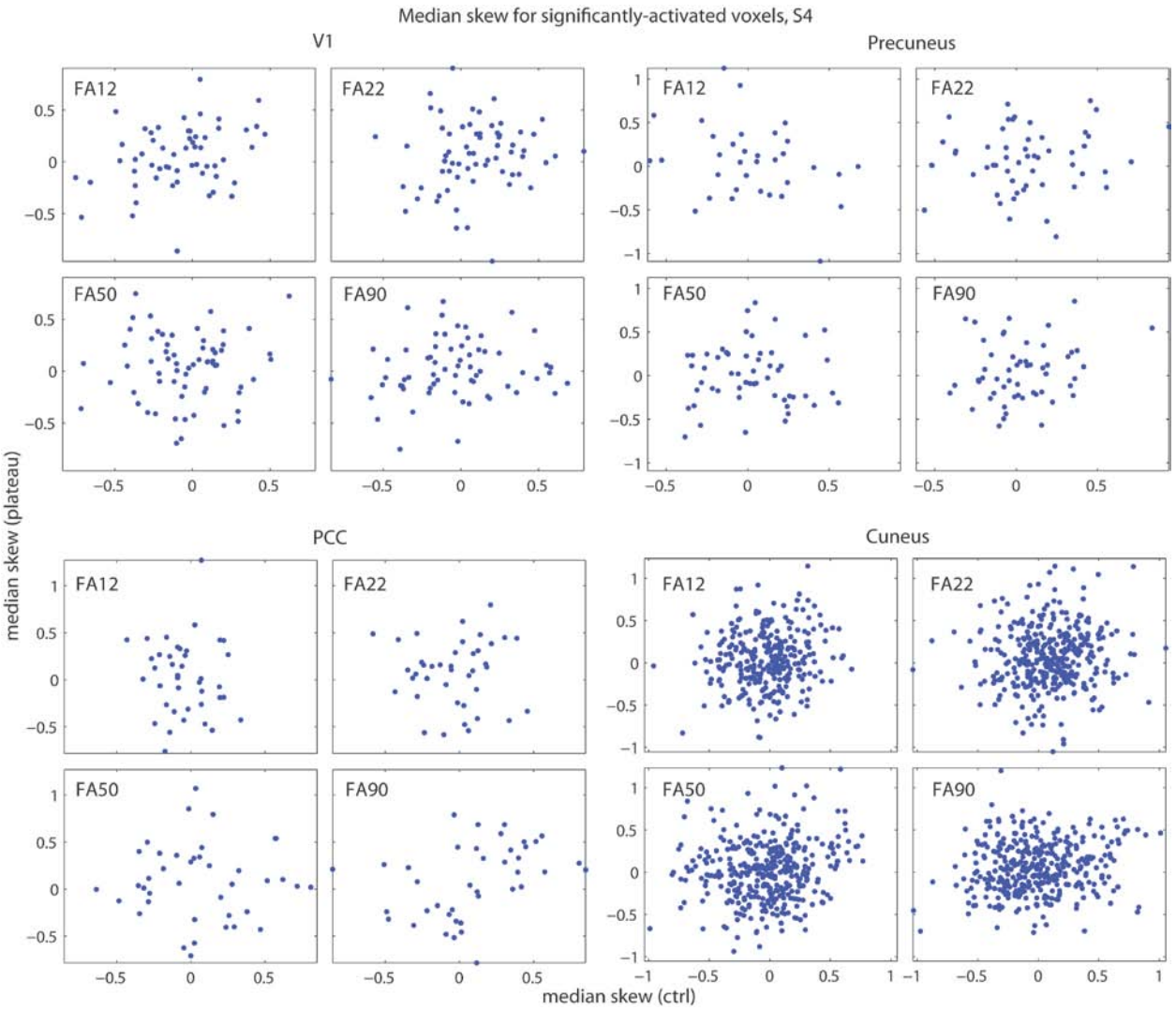

Fig. S4. Skewness of noise distributions between control and stimulation conditions in different ROIs and *FA*s. The points, representing individual voxels, include all of the statistically significantly responding voxels in a representative subject in each of the indicated ROIs. The scatter plots do not show any clear structure and look quite similar across *FA*s in each of the ROIs. We thus conclude that the *FA* does not produce any major skewness in the noise distribution independently of signal in the activation period. Consequently, the *FA* effects we observed in our data do not appear to be driven by processes that differentially affect the noise component of the signal.

Table S1: Proportional activation/deactivation in PCC. Number of significantly activated voxels in left PCC, cumulative across all subjects excluding the subject indicated at the top of the "Skip" row. Voxel counts in column "none" correspond to the cumulative sum across all subjects. Voxel counts are grouped by negative ($\beta < 0$) and positive ($\beta > 0$) significant correlations for FA12 only (second row) and FA90 only (third row), followed by commonly active voxels at both *FA*s (independent of the sign of β). The chi squared contingency test was performed on all subjects and by leaving one subject at a time out of the analysis. The last row reports the χ^2 value for contingency of the $\beta < 0$ and $\beta > 0$ proportions across the two *FA*s. The lowest χ^2 value (= 13.9) of the "leave one out" analysis corresponds to the highest *p*-value ($p < 0.0002$) in the χ^2 statistic with a single degree of freedom.

	Skip:								
	1	2	3	4	5	6	7	8	None
FA12 only									
$\beta < 0$	117	129	119	125	102	107	135	118	136
$\beta > 0$	26	21	27	26	23	18	23	25	27
FA90 only									
$\beta < 0$	76	66	42	79	80	74	53	79	80
$\beta > 0$	68	72	65	73	56	40	74	70	74
Common	120	122	61	125	104	100	124	126	126
χ^2	27.5	41.1	47.6	32.7	16.0	13.9	59.9	28.9	36.2

Table S2: Proportional activation/deactivation in cuneus. Number of voxels in left cuneus grouped in negative ($\beta < 0$) and positive ($\beta > 0$) significant correlations for FA12 only and FA90 only, followed by commonly active voxels (independent of the sign of β). See the caption of Table S1 for specifics of data presentation. The lowest χ^2 value (= 11.6) of the "leave one out" analysis corresponds to the highest *p*-value ($p < 0.0007$) in the χ^2 statistic.

	Skip:								
	1	2	3	4	5	6	7	8	none
FA12 only									
$\beta < 0$	76	125	106	138	133	132	139	131	140
$\beta > 0$	171	138	159	132	173	171	176	147	181
FA90 only									
$\beta < 0$	75	65	58	81	62	79	66	81	81
$\beta > 0$	319	401	385	393	344	346	354	370	416
Common	1458	1410	1342	1495	1364	1375	1588	1462	1642
χ^2	11.6	98.4	67.5	95.9	69.7	53.6	72.3	70.9	73.8

Table S3: Cumulative sum of activated voxels in seed analysis. **Left**. Number of positive and negative significantly activated voxels in the seed analysis for each left-hemisphere ROI and each *FA*. Voxel counts represent the cumulative sum across all 8 subjects except for left pSTG (subject 1 excluded because there were no significantly activated voxels for FA12). **Right**. Fraction of voxels in each *FA* condition relative to the number of voxels obtained from the FA12 condition.

ROI	FA12	FA22	FA50	FA90	Ratio FA12/		
					FA22	FA50	FA90
Cuneus							
Positive	1702	2101	2230	2074	0.81	0.76	0.82
Negative	149	229	145	103	0.65	1.03	1.45
Lingual gyrus							
Positive	2269	2718	2716	2559	0.83	0.83	0.89
Negative	81	85	65	50	0.95	1.25	1.62
Middle occipital gyrus							
Positive	1618	2078	2189	1959	0.78	0.74	0.83
Negative	18	22	11	4	0.82	1.64	4.50
Posterior cingulate cortex							
Positive	157	198	152	173	0.79	1.03	0.91
Negative	156	202	129	92	0.77	1.21	1.70
Precuneus							
Positive	180	261	263	271	0.69	0.68	0.66
Negative	180	186	112	94	0.97	1.61	1.91
Posterior superior temporal gyrus							
Positive	64	235	80	109	0.27	0.80	0.59
Negative	98	83	120	74	1.18	0.82	1.32